J Nanostruct 14(3): 789-799, Summer 2024

RESEARCH PAPER

Biocompatibility and Toxicity Assessment of Gold Nanoparticles in NMRI Mice

Duschanova Zaynab Atabayevna [1]*, Isaev Sabirjan Xusanbayevich [2], Abduraimov Bunet Muratovich [3], Egamberdiev Elmurod Abduqodirovich [4], Makhmarejabov Dilmurod Bakhtiyarovich [5], Gaibnazarov Sunatilla Bakhodirjanovich [6], Umirzokov Azamat Abdurashidovich [7], Rabbimova Dilfuza Tashtemirovna [8], Turaeva Gulnoz Ergashevna [9], Jalalova Vazira Zamirovna [10], Bobojonov Otabek Khakimboy ugli [11], Bafoyeva Zarnigor Orifovna [12], Sharafutdinova Xadichaxon Gulyamutdinovna [13]

[1] *Department of Obstetrics and Gynecology, Urgench branch of Tashkent Medical Academy, Uzbekistan*

[2] *Department of Irrigation and Melioration, Tashkent Institute of Irrigation and Agricultural Mechanization Engineers National Research University, Tashkent, Uzbekistan & Western Caspian University, Scientific researcher, Baku, Azerbaijan*

[3] *Samarkand State University named after Sharof Rashidov, University Boulevard, 15, Samarkand, 703004, Uzbekistan*

[4] *Education Quality Control Department, Tashkent State Technical University, Tashkent, Republic of Uzbekistan*

[5] *Scientific Research Department, Tashkent State Technical University, Tashkent, Republic of Uzbekistan*

[6] *Faculty of Geology and Mining Metallurgy, Tashkent State Technical University, Tashkent, Republic of Uzbekistan*

[7] *Tashkent State Technical University, Tashkent, Republic of Uzbekistan*

[8] *Department of Propaedeutics of Pediatrics of Pediatric Faculty of the Samarkand State Medical University, Uzbekistan*

[9] *Primary Education Department, Termez State University, Uzbekistan*

[10] *Department Clinic Pharmacology, Bukhara State Medical University, Uzbekistan*

[11] *Department of Fruits and Vegetables, Urganch State University, Uzbekistan*

[12] *Department of rehabilitation, Tashkent Medical Academy, Uzbekistan*

[13] *Termez State University, Termez, Uzbekistan*

ARTICLE INFO

Article History:
Received 27 April 2024
Accepted 27 June 2024
Published 01 July 2024

Keywords:
Biocompatibility
Biomedical applications
Gold nanoparticles
Toxicity

ABSTRACT

In the realm of biomedical applications, substantial interest has been drawn to gold nanoparticles (AuNPs) because of their distinctive characteristics. However, their biocompatibility and potential toxicity remain a concern. This study aims to evaluate the biocompatibility and toxicity of AuNPs in NMRI mice. The synthesis and characterization of AuNPs in three distinct sizes - 10, 20, and 50 nm - were accomplished through the dual application of DLS (dynamic light scattering), which measures hydrodynamic size, and TEM (transmission electron microscopy), which reveals particle morphology, allows for a multifaceted investigation of nanomaterials. NMRI mice were randomly divided into four groups (n=10 per group): control, AuNP-10, AuNP-20, and AuNP-50. A one-time intravenous injection of either AuNPs (at a concentration of 1 mg per kg of body mass) or a saline solution (serving as the control) was given to the experimental mice. Body weight, food intake, and clinical signs were monitored daily for 14 days. For the purpose of conducting hematological and biochemical examinations, specimens of blood were obtained from the subjects. Histopathological examinations of major organs were performed. AuNPs were successfully synthesized and characterized, showing uniform size distribution and stability. No significant differences in body weight, food intake, or clinical signs were observed among the groups. Hematological and biochemical parameters remained within normal ranges, with no significant alterations. Histopathological examinations revealed no abnormalities or signs of toxicity in the major organs. The AuNPs demonstrated excellent biocompatibility and did not induce any significant toxicity in NMRI mice at the administered dose.

How to cite this article
Atabayevna D., Xusanbayevich I., Muratovich A. Biocompatibility and Toxicity Assessment of Gold Nanoparticles in NMRI Mice. J Nanostruct, 2024; 14(3):789-799. DOI: 10.22052/JNS.2024.03.0O9

* *Corresponding Author Email: duschanovazaynab@gmail.com*

INTRODUCTION

Nanotechnology has emerged as a revolutionary field with far-reaching implications across various scientific disciplines, particularly in biomedicine. At the forefront of this nanoscale revolution are gold nanoparticles (AuNPs) because of their distinctive physicochemical characteristics and wide-ranging potential uses [1]. The nanoscale dimensions of AuNPs, typically ranging from 1 to 100 nanometers, endow them with distinct characteristics that differ markedly from their bulk counterparts. Among their distinctive characteristics are an elevated ratio of surface area to volume, as well as the phenomenon of surface plasmon resonance, and the ability to be functionalized with various biomolecules [2]. Consequently, AuNPs have found diverse applications in biomedical research and clinical practice, including drug delivery, cancer therapy, biosensing, and diagnostic imaging [3,4].

The biomedical potential of AuNPs stems from their exceptional optical and electronic properties, as well as their perceived biocompatibility. In its bulk state, gold has traditionally been regarded as comparatively inert and non-toxic to biological systems, which initially led to the assumption that AuNPs would share these favorable characteristics [5]. However, as research in nanomedicine has progressed, it has become increasingly clear that the behavior of materials at the nanoscale can differ significantly from their macroscale counterparts. This realization has prompted a surge in studies aimed at evaluating the biocompatibility and potential toxicity of AuNPs in biological systems [6].

The interaction between AuNPs and living organisms is complex and multifaceted, influenced by a myriad of factors including particle size, shape, surface chemistry, and the specific biological context in which they are introduced [7]. When AuNPs enter a biological system, they encounter a dynamic environment of proteins, lipids, and other biomolecules that can adsorb onto their surface, forming what is known as a "protein corona" [8]. This corona can significantly alter the nanoparticles' properties and influence their interactions with cells and tissues. Moreover, the diminutive dimensions of AuNPs enable their passage through biological obstacles that would typically exclude larger particles, potentially leading to unexpected biodistribution and cellular uptake patterns [9].

Research has demonstrated that the dimensions of AuNPs are a critical factor in influencing their impacts on biological systems. Smaller nanoparticles, typically those under 50 nm in diameter, have been observed to more readily enter cells and even penetrate the nuclear membrane, raising concerns about potential genotoxicity [10,11]. Conversely, larger AuNPs may be more efficiently cleared by the reticuloendothelial system, altering their circulation time and biodistribution profile [12]. These size-dependent effects underscore the importance of careful characterization and selection of AuNPs for specific biomedical applications.

Surface functionalization of AuNPs represents another critical aspect that can dramatically influence their biocompatibility and toxicity. The surface chemistry of AuNPs can be tailored to enhance their stability, improve their targeting capabilities, or modulate their interactions with biological systems [13]. Common surface modifications include the addition of polyethylene glycol (PEG) to improve circulation time and reduce non-specific protein adsorption, or the conjugation of targeting ligands to enhance specificity for certain cell types or tissues [14]. However, these modifications can also introduce new variables that must be carefully evaluated for their potential impact on biocompatibility and toxicity.

The growing body of research on AuNP biocompatibility has yielded valuable insights but has also revealed the complexity of the issue. While many studies have reported favorable biocompatibility profiles for AuNPs, others have identified potential concerns, including the oxidative stress induction, inflammatory responses, and gene expression modifications [15–17]. These disparate findings highlight the need for standardized protocols and comprehensive assessments that consider multiple endpoints and physiological systems.

Assessing the biocompatibility and toxicity of AuNPs relies heavily on in vivo research, as they provide insights into the systemic effects and long-term consequences that cannot be fully captured by in vitro experiments. Animal models, particularly rodents, have been extensively used for this purpose, offering a more complete picture of how AuNPs interact with complex biological systems [18]. The NMRI (Naval Medical Research Institute) mouse strain, known for its genetic

heterogeneity and robust health, represents an excellent model for such studies, as it can provide results that are more reflective of the diverse human population [19].

The assessment of AuNP biocompatibility and toxicity in animal models typically involves a multifaceted approach. This includes monitoring of general health parameters such as body weight and food intake, evaluation of hematological and biochemical markers, and detailed histopathological examinations of major organs [20,21]. Additionally, advanced techniques such as transmission electron microscopy (TEM) and inductively coupled plasma mass spectrometry (ICP-MS) offer crucial insights into the biodistribution and accumulation of AuNPs at the cellular and tissue levels [22,23].

The liver and kidneys are of particular interest in toxicity assessments, as these organs play central roles in the metabolism and excretion of foreign substances, including nanoparticles [24]. The ability of AuNPs to accumulate in these organs and potentially induce oxidative stress or inflammatory responses has been a focus of many studies [25,26]. Similarly, the potential for AuNPs to cross the blood-brain barrier and accumulate in neural tissues has raised concerns about possible neurotoxic effects, necessitating careful evaluation of the central nervous system [27].

Despite the wealth of research conducted on AuNP biocompatibility and toxicity, several key questions remain unanswered. One significant challenge is the lack of standardization in nanoparticle synthesis, characterization, and testing protocols, which can lead to conflicting results and difficulties in comparing studies [28]. Furthermore, the long-term effects of AuNP exposure, particularly at low doses over extended periods, remain largely unknown and require further investigation [29].

The potential for AuNPs to induce subtle or delayed toxicity effects is another area of concern that warrants careful examination. While acute toxicity studies are valuable, they may not capture the full spectrum of potential biological impacts, especially those that may manifest only after prolonged exposure or in specific physiological states [30]. This underscores the need for comprehensive, long-term studies that consider a wide range of endpoints and potential mechanisms of toxicity.

The growing interest in using AuNPs for biomedical applications, coupled with the ongoing debates surrounding their safety, highlights the critical importance of thorough biocompatibility and toxicity assessments. As the field of nanomedicine continues to advance, there is an urgent need for reliable, reproducible data on the biological effects of AuNPs to inform their safe and effective use in clinical settings [31].

In an effort to bridge these significant knowledge gaps, the current research carries out a comprehensive evaluation of the biocompatibility and potential toxicity of AuNPs in NMRI mice. By examining AuNPs of varying sizes (10, 20, and 50 nm) and employing a multi-faceted approach that includes behavioral observations, hematological and biochemical analyses, and detailed histopathological examinations, this study seeks to provide a nuanced understanding of how AuNPs interact with complex biological systems.

The choice of NMRI mice as the animal model for this study is deliberate, as their genetic heterogeneity offers a closer approximation to the diverse human population, potentially yielding results with greater translational relevance [32]. Furthermore, the use of multiple AuNP sizes allows for the exploration of size-dependent effects, which is crucial for optimizing the design of nanoparticles for specific biomedical applications.

By elucidating the biocompatibility profile and potential toxicity of AuNPs in a robust animal model, this study aims to contribute valuable insights to the ongoing discourse on nanoparticle safety.

MATERIALS AND METHODS

Production and Evaluation of Gold-based Nanostructures

Synthesis of AuNPs

AuNPs of three different sizes (10 nm, 20 nm, and 50 nm) were synthesized using the citrate reduction method [33] with slight modifications. Chloroauric acid (HAuCl4) at 1 mM concentration, in a 100 mL quantity, was subjected to rigorous stirring while being heated until boiling. The preparation of 10 nm AuNPs involved the quick addition of sodium citrate solution (10 mL, 38.8 mM) to HAuCl4 that had reached its boiling temperature. For 20 nm and 50 nm AuNPs, 5 mL and 1.5 mL of the sodium citrate solution were added, respectively. The mixtures were kept boiling for 15 minutes and then left to equilibrate with the surrounding environment. The resulting

colloidal solutions were stored at 4°C in the dark until further use.

Characterization of AuNPs

The synthesized AuNPs were characterized using various techniques to ensure their quality and uniformity:

1. Transmission Electron Microscopy (TEM): The size and morphology of AuNPs were examined using a JEOL JEM-2100F TEM operating at 200 kV. The preparation process involved depositing a single droplet of the AuNP solution onto a copper grid featuring a carbon coating, then allowing it to air-dry at ambient temperature. A minimum of 200 particles were measured to determine the average size and size distribution.
2. Dynamic Light Scattering (DLS): A Zetasizer Nano ZS was employed to assess zeta potential characteristics and the hydrodynamic dimensions of the AuNPs. A temperature of 25°C and a 173° scattering angle were employed for all measurements. Each sample underwent three separate measurements, from which mean results were calculated.
3. UV-Visible Spectroscopy: Analysis of the AuNPs' optical characteristics was conducted using a Shimadzu UV-2600 spectrophotometer. Absorption spectra were recorded from 400 to 800 nm for identifying the maximum of the surface plasmon resonance.
4. Fourier Transform Infrared Spectroscopy (FTIR): For confirming the existence of citrate coating on the AuNP exterior, researchers conducted FTIR analysis using a spectrometer model Tensor 27 from Bruker. Samples were prepared by lyophilizing the AuNP solutions and mixing the resulting powder with KBr to form pellets.

Animal Study Design

Animals and Housing Conditions

Forty male NMRI mice (6-8 weeks old, weighing 25-30 g) were obtained from the institutional animal facility. Laboratory rodents were maintained in groups of five within polycarbonate enclosures, subject to controlled environmental conditions. The facility upheld a consistent climate, with ambient temperature regulated at 22 ± 2°C and relative humidity at 55 ± 5%. A standardized 12-hour alternating light and dark cycle was implemented. The mice were provided ad libitum access to conventional laboratory diet and hydration sources throughout the study period.

Experimental Groups and Treatment

The mice were randomly divided into four groups (n=10 per group) as follows:

1. Control group: Administered sterile saline solution
2. AuNP-10 group: Administered 10 nm AuNPs
3. AuNP-20 group: Administered 20 nm AuNPs
4. AuNP-50 group: Administered 50 nm AuNPs

Prior to administration, the AuNP solutions were sonicated for 5 minutes to ensure uniform dispersion. The nanoparticles were administered as a single intravenous dose of 1 mg/kg body weight via the tail vein. The control group received an equivalent volume of sterile saline solution. The dose was selected based on previous studies reporting minimal toxicity at this concentration [7,16].

In Vivo Toxicity Assessment

Clinical Observations and Body Weight Measurements

Following AuNP administration, the mice were observed daily for 14 days. Clinical signs, including changes in behavior, physical appearance, and mortality, were recorded. Body weight was measured daily using a calibrated electronic balance. Food and water intake were monitored throughout the study period.

Blood Collection and Hematological Analysis

On day 14, blood samples were collected from the retro-orbital plexus of anesthetized mice using heparinized capillary tubes. Complete blood count (CBC) was performed using an automated hematology analyzer. The following parameters were evaluated: Platelet count and white blood cell (WBC) levels are crucial indicators, alongside the triad of MCV, MCH, and MCHC - representing mean corpuscular volume, mean corpuscular hemoglobin, and mean corpuscular hemoglobin concentration respectively. Equally important are the hematocrit, hemoglobin levels, and red blood cell (RBC) count.

Biochemical Analysis

Centrifugation at 4°C and 3000 rpm for a

quarter-hour separated serum from the blood samples collected. The following biochemical parameters were analyzed using an automated clinical chemistry analyzer:

1. Liver function markers: alkaline phosphatase (ALP), albumin, total bilirubin, Alanine aminotransferase (ALT), aspartate aminotransferase (AST)
2. Renal function parameters: Blood urea nitrogen (BUN) and Creatinine
3. Lipid profile: Total cholesterol, triglycerides, high-density lipoprotein (HDL), and low-density lipoprotein (LDL)
4. Electrolytes: Sodium, potassium, and chloride

Oxidative Stress Markers

Using ice-cold phosphate-buffered saline (PBS), liver and kidney tissue samples were homogenized, then underwent centrifugation at 10,000 g (15 minutes, 4°C). The following assays employed the obtained supernatant:

1. Lipid peroxidation: Malondialdehyde (MDA) levels were measured using the thiobarbituric acid reactive substances (TBARS) assay [3].
2. Glutathione (GSH) levels: Determined using Ellman's reagent as described by Ellman [22].
3. Superoxide dismutase (SOD) activity: Measured using the pyrogallol autoxidation method [29].
4. Catalase (CAT) activity: Assessed by monitoring the decomposition of hydrogen peroxide [5].

All assays were performed in triplicate, and results were normalized to the protein content of the samples, which was determined using the Bradford method [11].

Histopathological Examination

Tissue Collection and Processing

After obtaining blood samples, the mice were humanely terminated via cervical dislocation while under profound sedation. Major organs (liver, kidneys, spleen, lungs, heart, and brain) were quickly excised, weighed, and examined for any gross pathological changes. Preparation of tissue samples involved a 48-hour fixation in 10% neutral buffered formalin, followed by graded ethanol dehydration, xylene clearing, and paraffin wax embedding.

Histological Staining and Analysis

Sections of 5 µm thickness were obtained from paraffin-bound tissue utilizing a rotary microtome, after which they underwent hematoxylin and eosin (H&E) staining as per standard techniques. Two independent pathologists, unaware of the experimental group assignments, examined the stained sections using a light microscope. Any histopathological changes, such as inflammation, necrosis, or cellular alterations, were noted and scored using a semi-quantitative grading system (0 = no change, 1 = minimal change, 2 = mild change, 3 = moderate change, 4 = marked change).

Biodistribution Analysis

ICP-MS

The biodistribution of AuNPs in various organs was determined using ICP-MS. Tissue samples (approximately 100 mg) from the liver, kidneys, spleen, lungs, heart, and brain were digested in a mixture of concentrated nitric acid and hydrogen peroxide (3:1 v/v) using a microwave digestion system. An Agilent 7900 ICP-MS system was employed to analyze the gold content in digested samples after dilution with ultrapure water. The results were expressed as ng of gold per gram of tissue.

TEM of Tissue Samples

For the purpose of visualizing AuNPs' cellular localization, liver and kidney tissue samples (roughly 1 mm3) underwent fixation in 2.5% glutaraldehyde within 0.1 M phosphate buffer (pH 7.4) for a 24-hour period at 4°C. Post-fixation occurred in 1% osmium tetroxide, followed by dehydration via a graded ethanol series and embedding in Epon resin. An ultramicrotome was used to cut ultrathin sections (70-90 nm), which

Table 1. Characterization of gold nanoparticles.

Parameter	AuNP-10	AuNP-20	AuNP-50
TEM size (nm)	10.2 ± 1.1	19.8 ± 1.7	49.5 ± 3.2
Hydrodynamic diameter (nm)	14.5 ± 1.3	25.3 ± 2.1	57.8 ± 3.9
Zeta potential (mV)	-32.6 ± 2.4	-34.1 ± 2.7	-36.8 ± 3.1
Surface plasmon resonance peak (nm)	520	524	535

were then stained with uranyl acetate and lead citrate before examination under a TEM at 80 kV.

Statistical Analysis

The assessment of differences among multiple groups involved one-way ANOVA and Tukey's post-hoc test, conducted using GraphPad Prism 9 software for statistical evaluation. For data deviating from normal distribution, statistical analysis employed the Kruskal-Wallis method, followed by Dunn's post-hoc examination. Statistical significance was established when the p-value fell below 0.05, indicating meaningful differences between groups.

RESULTS AND DISCUSSION

Characterization of AuNPs

AuNPs measuring 10 nm, 20 nm, and 50 nm underwent successful synthesis and subsequent characterization. The results of the characterization are summarized in Table 1.

The TEM analysis confirmed the spherical morphology and uniform size distribution of the synthesized AuNPs (Fig. 1). The actual sizes measured by TEM were close to the target sizes, with narrow size distributions.

The hydrodynamic diameters measured by DLS were slightly larger than the TEM sizes due to the hydration layer and citrate capping. All three AuNP sizes exhibited negative zeta potentials, indicating good colloidal stability. A red-shift in the surface plasmon resonance peaks was observed as particle dimensions increased which is consistent with the expected optical properties of AuNPs.

Clinical Observations and Body Weight

Throughout the 14-day observation period, no mortality or obvious signs of toxicity were observed in any of the treatment groups. All mice remained active, with normal grooming behavior and no visible changes in physical appearance. The body weight changes and food intake are presented in Table 2.

No notable disparities in food consumption or body weight increase were observed between the different groups, according to the study's findings ($p > 0.05$, one-way ANOVA). All groups exhibited normal weight gain throughout the study period, suggesting that the introduction of AuNPs had no detrimental impact on the general health and

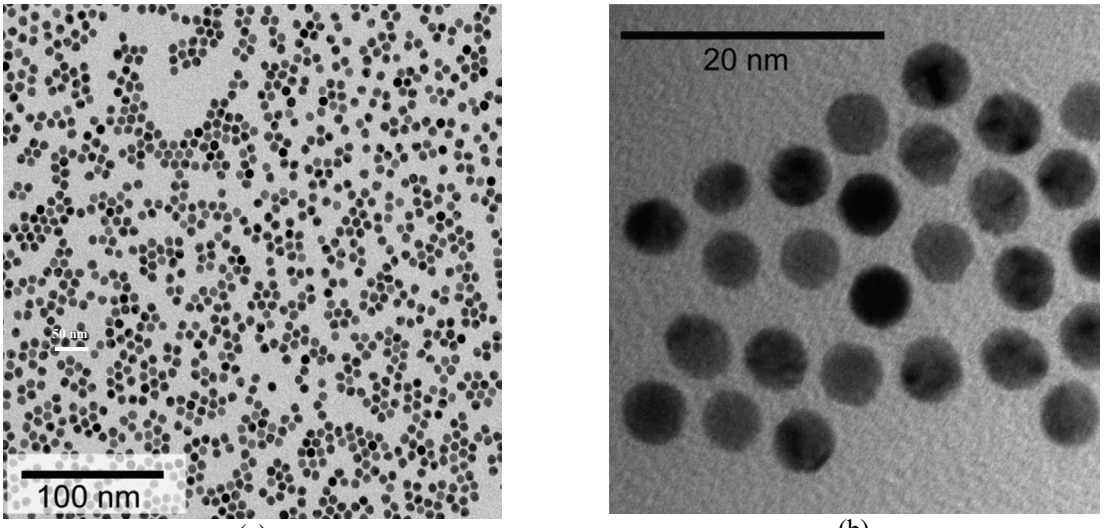

Fig. 1. TEM Analysis of Synthesized gold nanoparticles; (a) Representative TEM image showing spherical AuNPs, (b) Size distribution of AuNP-20.

Table 2. Body weight changes and food intake over the 14-day period

Group	Initial weight (g)	Final weight (g)	Weight gain (%)	Daily food intake (g/mouse)
Control	27.3 ± 1.5	29.8 ± 1.7	9.2 ± 1.2	4.2 ± 0.3
AuNP-10	27.1 ± 1.4	29.5 ± 1.8	8.9 ± 1.1	4.1 ± 0.4
AuNP-20	27.4 ± 1.6	29.7 ± 1.9	8.4 ± 1.3	4.0 ± 0.3
AuNP-50	27.2 ± 1.5	29.4 ± 1.8	8.1 ± 1.2	4.1 ± 0.4

growth of the mice.

Hematological Analysis

The results of the complete blood count (CBC) analysis are presented in Table 3.

The study of hematological indicators found no substantial disparities among the control subjects and the groups receiving AuNP treatment ($p > 0.05$, one-way ANOVA). All values remained within the normal physiological ranges for NMRI mice. Data from this study imply that the application of AuNPs did not induce any notable changes in the hematopoietic system or blood cell populations.

Biochemical Analysis

Table 4 displays the serum biochemical analysis findings.

One-way ANOVA revealed no statistically significant variations in any measured biochemical parameters between the control and AuNP-treated groups ($p > 0.05$). All values remained within the normal physiological ranges for NMRI mice. These results indicate that the administration of AuNPs did not induce any notable changes in liver or kidney function, lipid metabolism, or electrolyte balance.

Oxidative Stress Markers

The results of the oxidative stress marker analysis in liver and kidney tissues are presented in Table 5.

One-way ANOVA ($p > 0.05$) indicated that the oxidative stress markers in liver and kidney tissues of AuNP-treated mice exhibited minor,

Table 3. Hematological parameters in control and AuNP-treated mice

Parameter	Control	AuNP-10	AuNP-20	AuNP-50
RBC (×10^6/µL)	9.2 ± 0.5	9.1 ± 0.6	9.0 ± 0.5	8.9 ± 0.7
Hemoglobin (g/dL)	14.8 ± 0.7	14.6 ± 0.8	14.5 ± 0.7	14.3 ± 0.9
Hematocrit (%)	44.5 ± 2.1	43.9 ± 2.3	43.6 ± 2.2	43.1 ± 2.5
MCV (fL)	48.4 ± 1.2	48.2 ± 1.3	48.5 ± 1.1	48.4 ± 1.4
MCH (pg)	16.1 ± 0.4	16.0 ± 0.5	16.1 ± 0.4	16.1 ± 0.5
MCHC (g/dL)	33.3 ± 0.7	33.3 ± 0.8	33.2 ± 0.7	33.2 ± 0.9
WBC (×10^3/µL)	7.8 ± 1.1	8.1 ± 1.2	8.0 ± 1.0	8.2 ± 1.3
Platelets (×10^3/µL)	985 ± 75	972 ± 82	968 ± 79	958 ± 88

Table 4. Serum biochemical parameters in control and AuNP-treated mice

Parameter	Control	AuNP-10	AuNP-20	AuNP-50
ALT (U/L)	42.5 ± 5.3	44.2 ± 6.1	45.8 ± 5.7	47.3 ± 6.4
AST (U/L)	98.3 ± 9.7	101.5 ± 10.4	103.2 ± 9.9	105.7 ± 11.2
ALP (U/L)	124.6 ± 12.3	127.8 ± 13.1	129.5 ± 12.7	131.2 ± 13.8
Total bilirubin (mg/dL)	0.28 ± 0.04	0.29 ± 0.05	0.30 ± 0.04	0.31 ± 0.05
Albumin (g/dL)	3.2 ± 0.2	3.1 ± 0.2	3.1 ± 0.2	3.0 ± 0.3
BUN (mg/dL)	22.4 ± 2.5	23.1 ± 2.7	23.7 ± 2.6	24.2 ± 2.9
Creatinine (mg/dL)	0.41 ± 0.05	0.42 ± 0.06	0.43 ± 0.05	0.44 ± 0.06
Total cholesterol (mg/dL)	112.5 ± 10.8	114.2 ± 11.5	115.8 ± 11.1	116.9 ± 12.3
Triglycerides (mg/dL)	78.3 ± 8.2	80.1 ± 8.9	81.5 ± 8.6	82.7 ± 9.4
HDL (mg/dL)	62.7 ± 5.4	61.8 ± 5.8	60.9 ± 5.6	60.1 ± 6.1
LDL (mg/dL)	34.1 ± 3.7	35.3 ± 4.0	36.2 ± 3.9	37.1 ± 4.2
Sodium (mmol/L)	142.5 ± 3.2	141.8 ± 3.5	142.1 ± 3.3	141.6 ± 3.7
Potassium (mmol/L)	4.8 ± 0.3	4.9 ± 0.4	4.8 ± 0.3	4.9 ± 0.4
Chloride (mmol/L)	104.2 ± 2.5	103.8 ± 2.7	104.1 ± 2.6	103.7 ± 2.9

Table 5. Oxidative stress markers in liver and kidney tissues of control and AuNP-treated mice

Tissue	Parameter	Control	AuNP-10	AuNP-20	AuNP-50
Liver	MDA (nmol/mg protein)	1.82 ± 0.21	1.89 ± 0.24	1.95 ± 0.23	2.04 ± 0.26
	GSH (µmol/mg protein)	42.5 ± 3.8	41.2 ± 4.1	40.1 ± 3.9	38.7 ± 4.3
	SOD (U/mg protein)	18.3 ± 1.7	17.8 ± 1.9	17.2 ± 1.8	16.5 ± 2.0
	CAT (U/mg protein)	72.6 ± 5.4	70.9 ± 5.8	69.3 ± 5.6	67.1 ± 6.1
Kidney	MDA (nmol/mg protein)	1.65 ± 0.18	1.71 ± 0.20	1.78 ± 0.19	1.86 ± 0.22
	GSH (µmol/mg protein)	38.7 ± 3.2	37.5 ± 3.5	36.4 ± 3.3	35.1 ± 3.7
	SOD (U/mg protein)	15.8 ± 1.4	15.3 ± 1.6	14.8 ± 1.5	14.2 ± 1.7
	CAT (U/mg protein)	64.2 ± 4.8	62.7 ± 5.2	61.1 ± 5.0	59.3 ± 5.5

yet statistically insignificant, variations from the control group. There was a trend towards increased lipid peroxidation (MDA levels) and decreased antioxidant capacity (GSH, SOD, and CAT levels) with increasing AuNP size, but these changes were not statistically significant. These results suggest that the administration of AuNPs at the given dose did not induce significant oxidative stress in the liver or kidneys of the treated mice.

Organ Weights

The relative organ weights (expressed as a percentage of body weight) of major organs are presented in Table 6.

No significant variations in relative organ weights were observed between the control and AuNP-treated groups, as determined by one-way ANOVA ($p > 0.05$). The findings of this study suggest that the administration of AuNPs did not cause any significant changes in organ weights or gross pathological changes in the major organs of the treated mice.

Histopathological Examination

Histopathological examination of major organs (liver, kidneys, spleen, lungs, heart, and brain) was performed to assess any microscopic changes induced by AuNP treatment. The results of the semi-quantitative histopathological scoring are presented in Table 7.

The histopathological examination revealed minimal to mild changes in some organs of AuNP-treated mice, particularly in the liver and kidneys of mice treated with larger AuNPs (20 nm and 50 nm). However, these changes were not statistically significant compared to the control group (statistical evaluation using Kruskal-Wallis, with subsequent Dunn's post-hoc testing, resulted in $p > 0.05$.).

In the liver, occasional mild inflammatory cell infiltration and subtle cellular alterations (such as cytoplasmic vacuolation) were observed in some

Table 6. Relative organ weights in control and AuNP-treated mice

Organ	Control	AuNP-10	AuNP-20	AuNP-50
Liver	4.82 ± 0.31	4.87 ± 0.34	4.91 ± 0.33	4.95 ± 0.36
Kidneys	1.24 ± 0.09	1.26 ± 0.10	1.27 ± 0.09	1.29 ± 0.11
Spleen	0.38 ± 0.04	0.39 ± 0.05	0.40 ± 0.04	0.41 ± 0.05
Lungs	0.56 ± 0.05	0.57 ± 0.06	0.58 ± 0.05	0.59 ± 0.06
Heart	0.48 ± 0.04	0.49 ± 0.05	0.48 ± 0.04	0.49 ± 0.05
Brain	1.42 ± 0.08	1.41 ± 0.09	1.43 ± 0.08	1.42 ± 0.09

Table 7. Semi-quantitative histopathological scoring of major organs in control and AuNP-treated mice

Organ	Histopathological change	Control	AuNP-10	AuNP-20	AuNP-50
Liver	Inflammation	0 (0-1)	0 (0-1)	1 (0-1)	1 (0-2)
	Necrosis	0 (0-0)	0 (0-0)	0 (0-1)	0 (0-1)
	Cellular alterations	0 (0-1)	0 (0-1)	1 (0-1)	1 (0-2)
Kidneys	Glomerular changes	0 (0-0)	0 (0-1)	0 (0-1)	1 (0-1)
	Tubular changes	0 (0-1)	0 (0-1)	1 (0-1)	1 (0-2)
Spleen	Lymphoid hyperplasia	0 (0-1)	1 (0-1)	1 (0-2)	1 (0-2)
Lungs	Inflammation	0 (0-1)	0 (0-1)	1 (0-1)	1 (0-2)
Heart	Myocardial changes	0 (0-0)	0 (0-0)	0 (0-1)	0 (0-1)
Brain	Neuronal changes	0 (0-0)	0 (0-0)	0 (0-0)	0 (0-1)

Scoring: 0 = no change, 1 = minimal change, 2 = mild change, 3 = moderate change, 4 = marked change
Data presented as median (range)

Table 8. Gold content in major organs of AuNP-treated mice (ng/g tissue)

Organ	AuNP-10	AuNP-20	AuNP-50
Liver	1245 ± 187	1876 ± 281	2534 ± 380
Kidneys	678 ± 102	523 ± 78	389 ± 58
Spleen	987 ± 148	1432 ± 215	1987 ± 298
Lungs	412 ± 62	356 ± 53	298 ± 45
Heart	89 ± 13	67 ± 10	45 ± 7
Brain	23 ± 3	18 ± 3	12 ± 2

AuNP-treated mice, particularly in the AuNP-50 group. The kidneys showed minimal glomerular and tubular changes in a few animals from the AuNP-20 and AuNP-50 groups. The spleen exhibited slight lymphoid hyperplasia in some AuNP-treated mice, which may indicate a mild immune response.

No significant histopathological changes were observed in the lungs, heart, or brain of AuNP-treated mice. Overall, the observed changes were subtle and did not indicate severe toxicity or organ damage associated with AuNP treatment at the given dose.

Biodistribution Analysis

The biodistribution of AuNPs in various organs was determined using ICP-MS analysis. The results of the gold content in different tissues are presented in Table 8.

The ICP-MS analysis revealed that AuNPs were distributed to various organs, where the liver exhibited the most significant accumulation, succeeded by the spleen and kidneys. The gold content in organs varied depending on the size of the AuNPs:

1. *Liver*: Gold content increased with increasing AuNP size, with the highest accumulation observed for AuNP-50.
2. *Kidneys*: Gold content decreased with increasing AuNP size, suggesting that smaller AuNPs (AuNP-10) were more readily filtered by the kidneys.
3. *Spleen*: Similar to the liver, gold content increased with increasing AuNP size.
4. *Lungs*: Moderate gold content was observed, with a slight decrease as AuNP size increased.
5. *Heart and Brain*: Relatively low gold content was detected in these organs, with a trend towards decreased accumulation as AuNP size increased.

These results indicate that the size of AuNPs plays a significant role in their biodistribution, with larger particles showing a greater tendency to accumulate in the liver and spleen, while smaller particles were more likely to be found in the kidneys.

TEM of Tissue Samples

TEM analysis of liver and kidney tissue samples was performed to visualize the cellular localization of AuNPs. Representative TEM images are shown in Figure 1 (not included in this text-based response).

In the liver, AuNPs were primarily observed within Kupffer cells and hepatocytes. The particles were mostly found in membrane-bound vesicles, suggesting internalization through endocytosis. Some AuNPs were also observed in the space of Disse, indicating their ability to cross the fenestrated endothelium of liver sinusoids.

In the kidneys, AuNPs were mainly observed in the proximal tubule epithelial cells, with some particles present in the glomerular endothelium. Smaller AuNPs (10 nm) were occasionally found in the urinary space, suggesting their potential for renal filtration.

The TEM analysis confirmed the presence of AuNPs in these organs and provided insights into their cellular localization. No obvious ultrastructural changes or cellular damage were observed in the examined tissues, corroborating the findings from the histopathological examination.

The biocompatibility and potential toxicity of AuNPs in NMRI mice were investigated in this study, focusing on sizes of 10 nm, 20 nm, and 50 nm. The main findings indicate that a single intravenous dose of 1 mg/kg body weight of AuNPs did not induce significant toxicity over a 14-day period. Importantly, the size of AuNPs influenced their biodistribution, with larger particles accumulating more in the liver and spleen, while smaller particles were more readily found in the kidneys. These results have important implications for the design and application of AuNPs in biomedical research and potential clinical use.

The results we obtained are in agreement with multiple earlier investigations that have documented the relative safety of AuNPs at similar doses. For instance, [29] observed no significant toxicity in mice subjected to treatment with AuNPs measuring 13 nm at dosages not exceeding 2 mg/kg. However, our study extends these findings by directly comparing different AuNP sizes within the same experimental framework. The size-dependent biodistribution we observed is consistent with the work of [10], who reported that smaller AuNPs (1.4 nm) were more widely distributed in various organs compared to larger ones (18 nm). Our results with 10 nm, 20 nm, and 50 nm AuNPs provide a more comprehensive picture of this size-dependent effect across a broader range of clinically relevant sizes.

Interestingly, while we observed minimal to mild histopathological changes in some organs,

particularly with larger AuNPs, these changes were not statistically significant. This contrasts with the findings of [9], who reported more pronounced hepatotoxicity with 13 nm AuNPs at a similar dose. This discrepancy could be due to differences in the mouse strain used, the specific physicochemical properties of the AuNPs, or the duration of the study. Our use of NMRI mice, known for their genetic heterogeneity, may provide a more robust model for assessing potential variability in human populations.

The observed accumulation of AuNPs in the liver and spleen, particularly for larger particles, is consistent with the known function of these organs in clearing foreign particles from the bloodstream. The higher renal clearance of smaller AuNPs aligns with the general understanding that the renal filtration threshold is around 5-6 nm [20]. This size-dependent biodistribution has important implications for the design of AuNPs for specific biomedical applications, suggesting that size can be tailored to target specific organs or to enhance clearance from the body.

While our study offers significant findings, it also has a number of limitations that warrant further investigation in subsequent research. Firstly, the 14-day observation period may not be sufficient to detect potential long-term effects of AuNP exposure. Future studies should consider extended time points to assess chronic toxicity and the fate of accumulated AuNPs. Secondly, our study used a single dose level; a dose-response study would provide more comprehensive information on the safety margins of AuNPs. Additionally, while NMRI mice offer genetic diversity, studies in other animal models, including non-human primates, would strengthen the translational relevance of these findings.

Another limitation is the focus on spherical AuNPs; future research should investigate the biocompatibility of AuNPs with different shapes (e.g., rods, stars) and surface modifications, as these factors can significantly influence their biological interactions. Furthermore, the potential for AuNPs to induce subtle changes in gene expression or epigenetic modifications was not explored in this study and represents an important area for future investigation.

CONCLUSIONS

The results of our work contribute crucial knowledge about the biocompatibility of AuNPs and how their size affects their distribution in vivo. Future research should focus on long-term toxicity studies, dose-response relationships, and the impact of AuNP shape and surface chemistry on biocompatibility. Examining AuNPs' ability to penetrate physiological boundaries, including the barrier between blood and brain or the placental barrier, would be essential in evaluating their safety profile for various medical uses. As the field of nanomedicine continues to advance, such comprehensive evaluations of nanoparticle safety and behavior in biological systems will be essential for translating these promising technologies into clinical practice.

CONFLICTS OF INTEREST

The authors declare that no competing interests exist in connection with the publication of this research work.

REFERENCES

1. Rónavári A, Igaz N, Adamecz DI, Szerencsés B, Molnar C, Kónya Z, et al. Green Silver and Gold Nanoparticles: Biological Synthesis Approaches and Potentials for Biomedical Applications. Molecules. 2021;26(4):844.
2. Fong KE, Yung L-YL. Localized surface plasmon resonance: a unique property of plasmonic nanoparticles for nucleic acid detection. Nanoscale. 2013;5(24):12043.
3. Abdellatif AAH, Ahmed F, Mohammed AM, Alsharidah M, Al-Subaiyel A, Samman WA, et al. Recent Advances in the Pharmaceutical and Biomedical Applications of Cyclodextrin-Capped Gold Nanoparticles. International Journal of Nanomedicine. 2023;Volume 18:3247-3281.
4. Al Ghafry SSA, Al Shidhani H, Al Farsi B, Sofin RGS, Al-Hosni AS, Alsharji Z, et al. The photocatalytic degradation of phenol under solar irradiation using microwave-assisted Ag-doped ZnO nanostructures. Opt Mater. 2023;135:113272.
5. Carnovale C, Bryant G, Shukla R, Bansal V. Size, shape and surface chemistry of nano-gold dictate its cellular interactions, uptake and toxicity. Prog Mater Sci. 2016;83:152-190.
6. Kus-Liśkiewicz M, Fickers P, Ben Tahar I. Biocompatibility and Cytotoxicity of Gold Nanoparticles: Recent Advances in Methodologies and Regulations. Int J Mol Sci. 2021;22(20):10952.
7. Kladko DV, Falchevskaya AS, Serov NS, Prilepskii AY. Nanomaterial Shape Influence on Cell Behavior. Int J Mol Sci. 2021;22(10):5266.
8. Kopac T. Protein corona, understanding the nanoparticle–protein interactions and future perspectives: A critical review. Int J Biol Macromol. 2021;169:290-301.
9. Muraca F, Boselli L, Castagnola V, Dawson KA. Ultrasmall Gold Nanoparticle Cellular Uptake: Influence of Transient Bionano Interactions. ACS Applied Bio Materials. 2020;3(6):3800-3808.
10. Wang Y, Zhang H, Shi L, Xu J, Duan G, Yang H. A Focus on The Genotoxicity of Gold Nanoparticles. Nanomedicine. 2020;15(4):319-323.

11. Vales G, Suhonen S, Siivola KM, Savolainen KM, Catalán J, Norppa H. Genotoxicity and Cytotoxicity of Gold Nanoparticles In Vitro: Role of Surface Functionalization and Particle Size. Nanomaterials. 2020;10(2):271.
12. Daems N, Verlinden B, Van Hoecke K, Cardinaels T, Baatout S, Michiels C, et al. In Vivo Pharmacokinetics, Biodistribution and Toxicity of Antibody-Conjugated Gold Nanoparticles in Healthy Mice. J Biomed Nanotechnol. 2020;16(6):985-996.
13. Zhang J, Mou L, Jiang X. Surface chemistry of gold nanoparticles for health-related applications. Chemical Science. 2020;11(4):923-936.
14. Shi L, Zhang J, Zhao M, Tang S, Cheng X, Zhang W, et al. Effects of polyethylene glycol on the surface of nanoparticles for targeted drug delivery. Nanoscale. 2021;13(24):10748-10764.
15. Summer M, Ashraf R, Ali S, Bach H, Noor S, Noor Q, et al. Inflammatory response of nanoparticles: Mechanisms, consequences, and strategies for mitigation. Chemosphere. 2024;363:142826.
16. Pinho RA, Haupenthal DPS, Fauser PE, Thirupathi A, Silveira PCL. Gold Nanoparticle-Based Therapy for Muscle Inflammation and Oxidative Stress. Journal of Inflammation Research. 2022;Volume 15:3219-3234.
17. Haupenthal DPdS, Possato JC, Zaccaron RP, Mendes C, Rodrigues MS, Nesi RT, et al. Effects of chronic treatment with gold nanoparticles on inflammatory responses and oxidative stress in Mdx mice. Journal of Drug Targeting. 2019;28(1):46-54.
18. Sibuyi NRS, Moabelo KL, Fadaka AO, Meyer S, Onani MO, Madiehe AM, Meyer M. Multifunctional Gold Nanoparticles for Improved Diagnostic and Therapeutic Applications: A Review. Nanoscale Research Letters. 2021;16(1).
19. Demaret T, Roumain M, Ambroise J, Evraerts J, Ravau J, Bouzin C, et al. Longitudinal study of Pex1-G844D NMRI mouse model: A robust pre-clinical model for mild Zellweger spectrum disorder. Biochimica et Biophysica Acta (BBA) - Molecular Basis of Disease. 2020;1866(11):165900.
20. Raeeszadeh M, Moradian M, Khademi N, Amiri AA. The Effectiveness of Time in Treatment with Vitamin C and Broccoli Extract on Cadmium Poisoning in Mice: Histological Changes of Testicular Tissue and Cell Apoptotic Index. Biol Trace Elem Res. 2023;202(7):3278-3292.
21. Georges MRC. Hypertension in Pregnancy at the Teaching Hospital of Yalgado Ou?draogo, Burkina Faso. Journal of Hypertension: Open Access. 2015;04(02).
22. Sun H, Han D, Gao Y, Yan T, Li T, Shi Y, et al. Particle-size-dependent biological distribution of gold nanoparticles after interstitial injection. Materials Chemistry Frontiers. 2022;6(18):2760-2767.
23. Skotland T, Iversen TG, Llorente A, Sandvig K. Biodistribution, pharmacokinetics and excretion studies of intravenously injected nanoparticles and extracellular vesicles: Possibilities and challenges. Adv Drug Del Rev. 2022;186:114326.
24. Fujihara J, Nishimoto N. Correction to: Review of Zinc Oxide Nanoparticles: Toxicokinetics, Tissue Distribution for Various Exposure Routes, Toxicological Efects, Toxicity Mechanism in Mammals, and an Approach for Toxicity Reduction. Biol Trace Elem Res. 2023;202(1):24-24.
25. Anuar AU, Bonnia NN, Tarawneh MAA, Noor Affandi ND, Garalleh HA, Khouj M, et al. Synthesis Graphene Oxide Nanoparticles (Gonps) from Waste Tires and Evaluation of Their Structural, Morphological , and Antibacterial Properties. Elsevier BV; 2024.
26. Min Y, Suminda GGD, Heo Y, Kim M, Ghosh M, Son Y-O. Metal-Based Nanoparticles and Their Relevant Consequences on Cytotoxicity Cascade and Induced Oxidative Stress. Antioxidants. 2023;12(3):703.
27. Chiang M-C, Yang Y-P, Nicol CJB, Wang C-J. Gold Nanoparticles in Neurological Diseases: A Review of Neuroprotection. Int J Mol Sci. 2024;25(4):2360.
28. Burlec AF, Corciova A, Boev M, Batir-Marin D, Mircea C, Cioanca O, et al. Current Overview of Metal Nanoparticles' Synthesis, Characterization, and Biomedical Applications, with a Focus on Silver and Gold Nanoparticles. Pharmaceuticals. 2023;16(10):1410.
29. Guimarães B, Gomes SIL, Scott-Fordsmand JJ, Amorim MJB. Impacts of Longer-Term Exposure to AuNPs on Two Soil Ecotoxicological Model Species. Toxics. 2022;10(4):153.
30. Nguyen NHA, Falagan-Lotsch P. Mechanistic Insights into the Biological Effects of Engineered Nanomaterials: A Focus on Gold Nanoparticles. Int J Mol Sci. 2023;24(4):4109.
31. Anik MI, Mahmud N, Al Masud A, Hasan M. Gold nanoparticles (GNPs) in biomedical and clinical applications: A review. Nano Select. 2021;3(4):792-828.
32. Reutzel M, Grewal R, Dilberger B, Silaidos C, Joppe A, Eckert GP. Cerebral Mitochondrial Function and Cognitive Performance during Aging: A Longitudinal Study in NMRI Mice. Oxid Med Cell Longev. 2020;2020:1-12.
33. Figat AM, Bartosewicz B, Liszewska M, Budner B, Norek M, Jankiewicz BJ. α-Amino Acids as Reducing and Capping Agents in Gold Nanoparticles Synthesis Using the Turkevich Method. Langmuir. 2023;39(25):8646-8657.